



LRRK2 deficiency protects the heart against myocardial infarction injury in mice via the P53/HMGB1 pathway

Yuan Liu¹, Lu Chen¹, Lu Gao¹, Xiaoxin Pei, Zekai Tao, Yawei Xu, Ran Li^{*}

Department of Cardiology, The First Affiliated Hospital of Zhengzhou University, Zhengzhou, China

ARTICLE INFO

Keywords:

Myocardial infarction
LRRK2
Hypoxia
P53
HMGB1

ABSTRACT

LRRK2 is a Ser/Thr kinase with multiple functional domains. Studies have shown that LRRK2 mutations are closely related to hereditary Parkinson's disease. However, its role in cardiovascular disease, especially in myocardial infarction, is unclear. The aim of this study was to explore the functional role of LRRK2 in myocardial infarction. Wild-type and LRRK2-knockout mice were subjected to coronary artery ligation (left anterior descending) to establish a myocardial infarction model. Neonatal rat cardiomyocytes were subjected to hypoxia to induce hypoxic injury *in vitro*. We found increased LRRK2 expression levels in the infarct periphery in mouse hearts and hypoxic cardiomyocytes. LRRK2-deficient mice exhibited decreased death rates and reduced infarction areas compared to wild-type controls 14 days after infarction. LRRK2-deficient mice showed reduced left ventricular fibrosis and inflammatory responses, as well as improved cardiac function. In the *in vitro* study, LRRK2 silencing decreased cleaved caspase-3 activity, reduced cardiomyocyte apoptosis, and diminished hypoxia-induced inflammation. However, LRRK2 overexpression enhanced cleaved caspase-3 activity, increased the number of apoptotic cardiomyocytes, and caused remarkable hypoxia-induced inflammation. When examining the underlying mechanisms, we found that hypoxia increased HIF α expression, which enhanced LRRK2 expression. LRRK2 induced high expression of HMGB1 via P53. When HMGB1 was blocked using an anti-HMGB1 antibody, the deleterious effects caused by LRRK2 overexpression following hypoxia were inhibited in cardiomyocytes. In summary, LRRK2 deficiency protects the heart against myocardial infarction injury. The mechanism underlying this effect involves the P53-HMGB1 pathway.

1. Introduction

According to data reported by the World Health Organization in 2016, cardiovascular diseases (CVDs) accounted for 31% of all mortality in 2016, and remain the leading cause of death [1]. An important contributing factor is myocardial infarction (MI) and heart failure induced by cardiac remodelling after acute MI (AMI) [2,3]. When the main branch of the coronary artery is suddenly occluded, cardiomyocytes undergo ischaemia or infarction. This process is called AMI, which eventually causes cardiomyocyte death and cardiac dysfunction [4]. With the development of revascularization techniques, the AMI survival rate continues to increase each year, which causes an increasing prevalence of heart failure (HF) [5]. After AMI, many cardiomyocytes undergo necrosis and apoptosis, causing a diverse range of immune cells to be recruited into the infarcted heart, where they engulf

dead cardiomyocytes and release various proinflammatory and profibrotic cytokines [6]. These cytokines promote an inflammatory cascade reaction and fibrotic proliferation, leading to cardiac systolic and diastolic dysfunction and ultimately HF [7]. Despite increased awareness of these processes and the development of various interventions, the overall mortality rate due to acute myocardial infarction-induced HF remains high, and more effective treatment strategies are needed [8].

When the heart experiences ischaemic injury, the ubiquitous protein high mobility group box 1 (HMGB1) can be released from necrotic cardiomyocytes and actively secreted by stressed cells [9]. HMGB1 is a typical damage-associated molecular pattern (DAMP) that binds to various receptors and signalling molecules, such as rage and Toll-like receptor (TLR)2/4, and induces the activation of NF- κ B and extracellular signal-regulated kinase (ERK) 1/2 signalling, triggering cells to produce proinflammatory cytokines [10,11]. In many cardiovascular

^{*} Corresponding author. Department of Cardiology, The First Affiliated Hospital of Zhengzhou University, No.1 Jianshe East Road, Zhengzhou, 450052, China.
E-mail addresses: fccliuy2@zzu.edu.cn (Y. Liu), 202012402015924@gs.zzu.edu.cn (L. Chen), gaomei1215@163.com (L. Gao), peixiaoxin1995@163.com (X. Pei), 1113679069@qq.com (Z. Tao), xuyawei105@163.com (Y. Xu), fccliuy@zzu.edu.cn (R. Li).

¹ Yuan Liu, Lu Chen and Lu Gao have contributed equally to this work.

<https://doi.org/10.1016/j.freeradbiomed.2022.08.035>

Received 24 March 2022; Received in revised form 16 August 2022; Accepted 27 August 2022

Available online 30 August 2022

0891-5849/© 2022 The Authors. Published by Elsevier Inc. This is an open access article under the CC BY-NC license (<http://creativecommons.org/licenses/by-nc/4.0/>).

diseases, especially cardiac ischaemic injury, HMGB1 plays an essential role in disease development [12,13]. HMGB1 increases the expression of endothelial cell chemokine receptors and promotes the release of inflammatory factors, thereby inducing myocardial cell necrosis or apoptosis [14]. HMGB1 blockade can ameliorate cardiac fibrosis in experimental autoimmune myocarditis [15]. Therefore, HMGB1 is a therapeutic target for treating heart damage.

Leucine-rich repeat kinase 2 (LRRK2) is a Ser/Thr kinase with multiple functional domains that is implicated in Parkinson's disease (PD) [16]. LRRK2 is widely expressed in a variety of tissue types including brain, heart, lung, intestine [17–19]. The LRRK2 protein contains a Ras complex guanosine triphosphate hydrolase domain and a C-terminal Roc domain. Previous studies have focused on the functional role of LRRK2 in PD and other cerebrocortical diseases [16,20]. LRRK2 was also reported to be involved in paraquat-induced inflammatory sickness and the stress phenotype [21]. Gu S et al. reported that LRRK2 down-regulation inhibited cholangiocarcinoma development [22] and promoted thyroid cancer cell apoptosis [23]. LRRK2 has also been reported to participate in mitochondrial Ca^{2+} efflux and function [24]. And our previous study has found that LRRK2 acted a role in pressure overload induced cardiac hypertrophy and LRRK2 could directly regulate autophagy in cardiomyocytes [19]. Thus, LRRK2 may also participate in the progress of myocardial infarction. In this study, we established an MI model and used LRRK2 silencing to explore the functional role of LRRK2 in the progress of MI.

2. Materials and methods

2.1. Animals

The animal protocols were approved by the Animal Care and Use Committee of Zhengzhou University, and all the procedures performed according to the Guidelines for the Care and Use of Laboratory Animals published by the United States National Institutes of Health (NIH Publication, revised 2011). LRRK2-knockout (KO) mice were purchased from Jackson Laboratory (Jackson Laboratory, 016121). Wild-type littermates were used as controls. Male mice (8–10 weeks; 24–28 g) were subjected to left coronary artery ligation surgery. Fourteen days after surgery, the mice were sacrificed, and their hearts were removed.

2.2. Left coronary artery ligation surgery

Mice were anaesthetized with sodium pentobarbital (50 mg/kg, i.p.). After the pericardium was opened, a 7–0 silk suture was used to ligate the proximal left coronary descending artery (LAD) under the tip of the left atrial appendage. In the sham group, a 7–0 silk suture only encircled the LAD without ligation. After the chest was closed, 0.1 ml of 0.5% bupivacaine (Sigma–Aldrich) was injected into the mice to alleviate postoperative pain. The surgery was performed in a blinded manner.

2.3. Echocardiography and haemodynamics

Echocardiography and haemodynamic parameters were measured as described in our previous study [25,26]. Isoflurane (1.5%) was used to anaesthetize the mice. A MyLab 30CV ultrasound (Biosound Esaote) with a 10-MHz linear array ultrasound transducer was used to examine echocardiography parameters. For haemodynamic measurements, a microtip catheter transducer (SPR-839; Millar Instruments, Houston, TX, USA) was inserted into the right carotid artery and then advanced into the left ventricle (LV). A Millar Pressure-Volume System (MPVS-400; Millar Instruments) was used to record the data. PVAN data analysis software was used for the analysis.

2.4. Histological analysis, immunohistochemistry, and TUNEL staining

The mouse heart sections were embedded in paraffin and cut into 4-

to 5-mm thick sections. Haematoxylin and eosin (HE) and picric acid red (PSR) staining were performed as described in our previous study [25, 26]. The infarct size is expressed as a percentage of the total LV area. A single myocyte was measured using a quantitative digital image analysis system (Image-Pro Plus, version 6.0). For immunohistochemistry, the following primary antibodies were used: anti-CD68 (ABD Serotec, MCA1957) and anti-CD45 (Abcam, ab10558). A commercial kit was used to perform TUNEL staining and examine apoptotic cells (Millipore, USA, #S7111). A fluorescence microscope (Olympus DX51) was used to capture images.

2.5. Quantitative real-time polymerase chain reaction (RT-PCR) and western blot analysis

Total RNA was extracted from frozen mouse heart tissue and cardiomyocytes. RNA (2 µg per sample) was reverse transcribed into cDNA using oligonucleotide (DT) primers and a transcript first strand cDNA synthesis kit (Roche). Then, we used a Light Cycler 480 instrument (software version 1.5, Roche) to perform PCR analysis using SYBR green PCR master mix (Roche). GAPDH was used as the internal reference gene.

Heart tissues and cardiomyocytes were lysed in RIPA lysis buffer. Protein samples (50 µg) were separated by SDS–PAGE and transferred to a PVDF membrane (Millipore, Beijing, China), which was then incubated with different primary antibodies, including LRRK2, phosphorylated (P-)–P53, HMGB1 (purchased from Abcam, 1:1000 dilution), and GAPDH (purchased from Cell Signaling Technology, 1:1000 dilution). The blots were developed with enhanced chemiluminescence (ECL) reagents (Bio–Rad, Hercules, CA, USA) and captured by a ChemiDoc MP Imaging System (Bio–Rad). GAPDH (Santa Cruz) served as an internal reference protein.

2.6. Cell culture

Neonatal rat cardiomyocytes (NRCMs) were isolated as described previously [25]. Sprague–Dawley rat (1- to 3-day-old)-derived NRCMs were seeded (1×10^6 cells/well) into six-well plates in DMEM/F12 with 10% foetal bovine serum (FBS). 5-Bromo-2-deoxyuridine (0.1 mM; BrdU, Sigma, B5002) was used to suppress fibroblast growth. Then, the cells were serum-starved for 8 h, transfected with si-LRRK2 (Santa Cruz) or the negative control (ScrNA), and then subjected to hypoxia for 24 h. The hypoxia model was established as described previously [27]. The cells were transfected with adenovirus (Ad-)LRRK2 (Vigene, Shangdong, China) for 8 h to overexpress LRRK2. The cells were then treated with an HMGB1-specific neutralizing antibody (50 µg/ml, ST326052233; Shinno-Test, Tokyo, Japan) for 8 h to block HMGB1. Finally, the cells were treated with KC7F2 (20 µM, MedChemExpress) for 24 h to inhibit HIF-1α. Cells were also transfected with Ad-LRRK2 D1994A (kinase dead) (Vigene, Shangdong, China).

2.7. ELISA analysis and C-caspase-3 activity

ELISA kits (BioLegend) were used to measure the release of tumour necrosis factor (TNF)-α, interleukin (IL)-1, and IL-6 according to a previous study [28]. An ELISA plate reader (Synergy HT, BioTek, VT, USA) was used to measure the optical density of the samples at 450 nm. An HMGB1 ELISA kit (Cloud Clone, Wuhan, China) was used to measure HMGB1 concentrations in heart tissues and cardiomyocytes.

C-caspase-3 activity (Beyotime Biotech, China) was examined by a commercial assay according to the manufacturer's instructions.

2.8. Luciferase reporter assay

The synthesized promoter regions (from –2095 to –1-bp relative to the translation start site) of the LRRK2 gene were subcloned into the luciferase reporter vector (Promega, USA). Luciferase reporter

constructs were packed with an adenoviral system and then cotransfected into NRCMs with a control plasmid, followed by the indicated stimulation: HIF-1 α siRNA for 48 h. Then, the cells were harvested and lysed, and the luciferase activity was determined with the Dual-Luciferase Reporter Assay Kit (Promega, USA) according to the manufacturer's instructions. The PGL3 basic vector was used as a negative control.

2.9. Statistical analysis

The data are expressed as the mean \pm SD. The unpaired Student's *t*-test was used to compare differences between two groups. One-way ANOVA was used to compare differences between more than two groups. *P* values < 0.05 were considered statistically significant.

3. Results

3.1. Expression level of LRRK2 in ischaemic hearts and cardiomyocytes

To determine whether LRRK2 participates in MI pathology, we examined the mRNA and protein levels of LRRK2 at 3, 7, and 14 days after MI in mice. The results showed an increasing trend in the mRNA and protein levels of LRRK2 in heart tissue at 3, 7, and 14 days after MI (Fig. 1A–C). We then examined the expression of LRRK2 in cardiomyocytes. As shown in Fig. 1 D–F, the mRNA and protein levels of LRRK2 were sharply upregulated in hypoxic cardiomyocytes (24 h).

3.2. LRRK2 silencing relieves hypoxic cardiomyocyte injury

We then isolated NRCMs to perform the *in vitro* study. Three LRRK2 siRNA was designed to knockdown LRRK2 as shown in Fig. S1, only

siRNA2 and siRNA3 showed the knockdown efficiency. We also detected the effects of LRRK2 siRNA2 and siRNA3 and found that LRRK2 siRNA3 showed better protective effects as evidenced by increased cell viability and reduced caspase3 activity (Fig. S1 B and C). Thus NRCMs were transfected with LRRK2 siRNA3 and the negative control ScRNA to knock down LRRK2 (Fig. 2A). An MTT assay was used to examine cell viability after 24 h of hypoxia. NRCMs in the hypoxia group had reduced viability and an increased number of TUNEL-positive cells. NRCMs transfected with LRRK2 siRNA had higher viability and fewer TUNEL-positive cell numbers than cells transfected with ScRNA under hypoxic conditions (Fig. 2B and C). We then examined the activity of cleaved-caspase3 (c-caspase3), which is an apoptotic effector. As shown in Fig. 2D, hypoxia sharply increased c-caspase3 expression and activity compared to normoxia. LRRK2 knockdown abrogated this increase in c-caspase3 activation (Fig. 2D). As inflammation is a key feature in cardiomyocyte hypoxic injury, we examined the release of proinflammatory cytokines. As shown in Fig. 2E, the increased release of TNF α , IL-1, and IL-6 was downregulated by LRRK2 silencing.

3.3. LRRK2 overexpression deteriorates hypoxic cardiomyocyte injury

To explore whether LRRK2 overexpression caused deleterious effects, NRCMs were transfected with Ad-LRRK2 to induce LRRK2 overexpression (Fig. 3A). Contrary to the results shown in the LRRK2 siRNA experiments, LRRK2 overexpression decreased cell viability and increased TUNEL-positive cell numbers during hypoxic conditions compared to the negative control Ad-NC (Fig. 3B and C). The C-caspase3 staining and activity results were also consistent with the previous results. LRRK2 overexpression increased C-caspase3 expression and activation under hypoxic conditions compared to those in the Ad-NC group (Fig. 3D). The release of TNF α , IL-1, and IL-6 in the Ad-LRRK2 group was

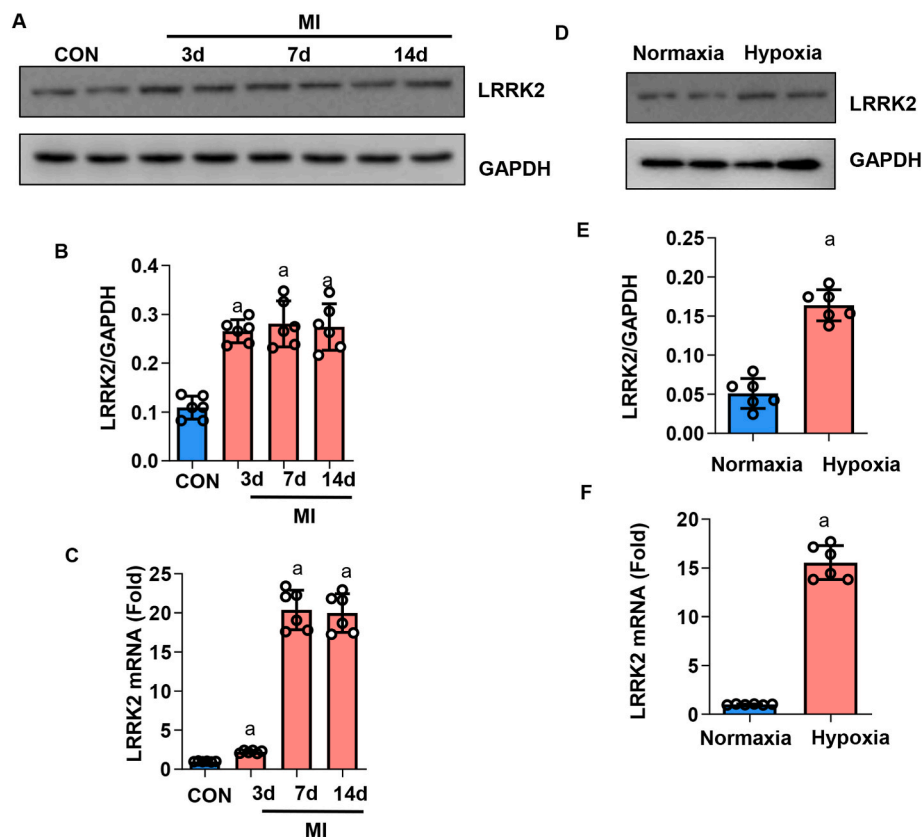


Fig. 1. Expression level of LRRK2 in ischaemic hearts and cardiomyocytes

A and B. Protein levels of LRRK2 in hearts after MI (n = 6). C. mRNA levels of LRRK2 in hearts after MI (n = 6). C and D. Protein levels of LRRK2 in NRCMs after 24 h of hypoxia (n = 6). F. mRNA levels of LRRK2 in NRCMs. ^a*P* < 0.05 vs. the CON/Normoxia group.

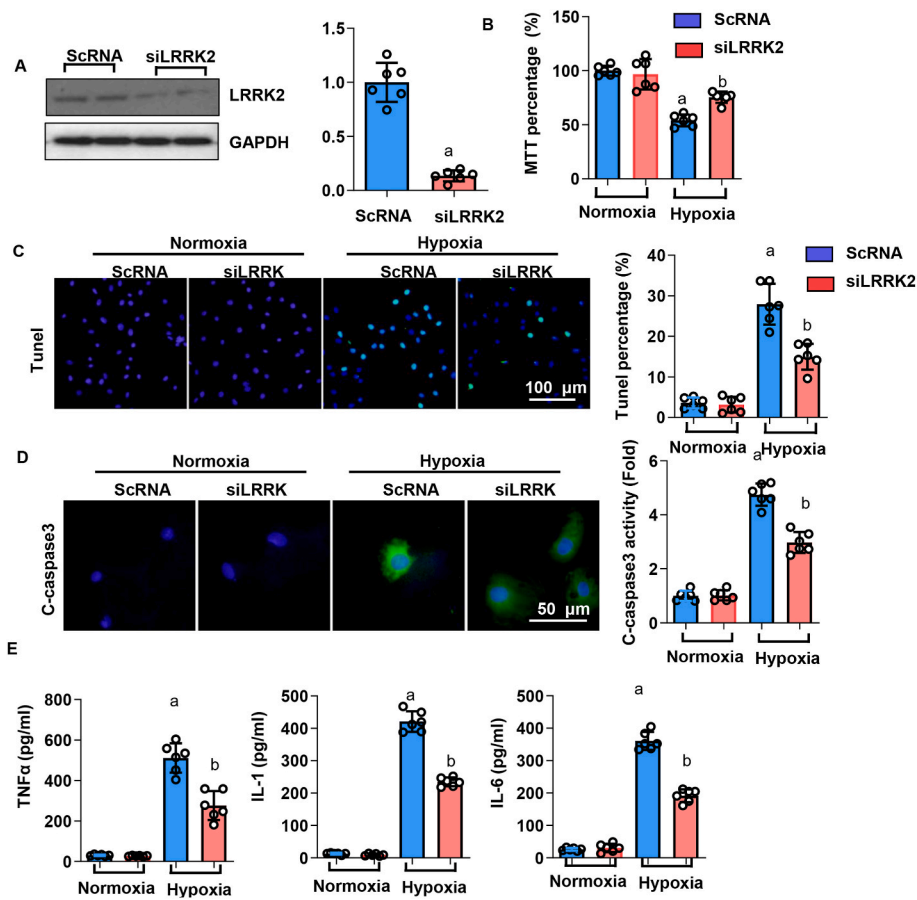


Fig. 2. LRRK2 silencing relieves hypoxic cardiomyocyte injury
 A. Protein expression of LRRK2 in NRCMs after transfection with LRRK2 siRNA (n = 6). B. Cell viability after hypoxia for 24 h (n = 6). C. TUNEL staining and quantified results (n = 5). D. C-caspase3 staining and activity (n = 6). F. ELISA analysis of proinflammatory cytokine concentrations (n = 6). ^aP < 0.05 vs. the Normoxia-ScRNA group, ^bP < 0.05 vs. the hypoxia-ScRNA group.

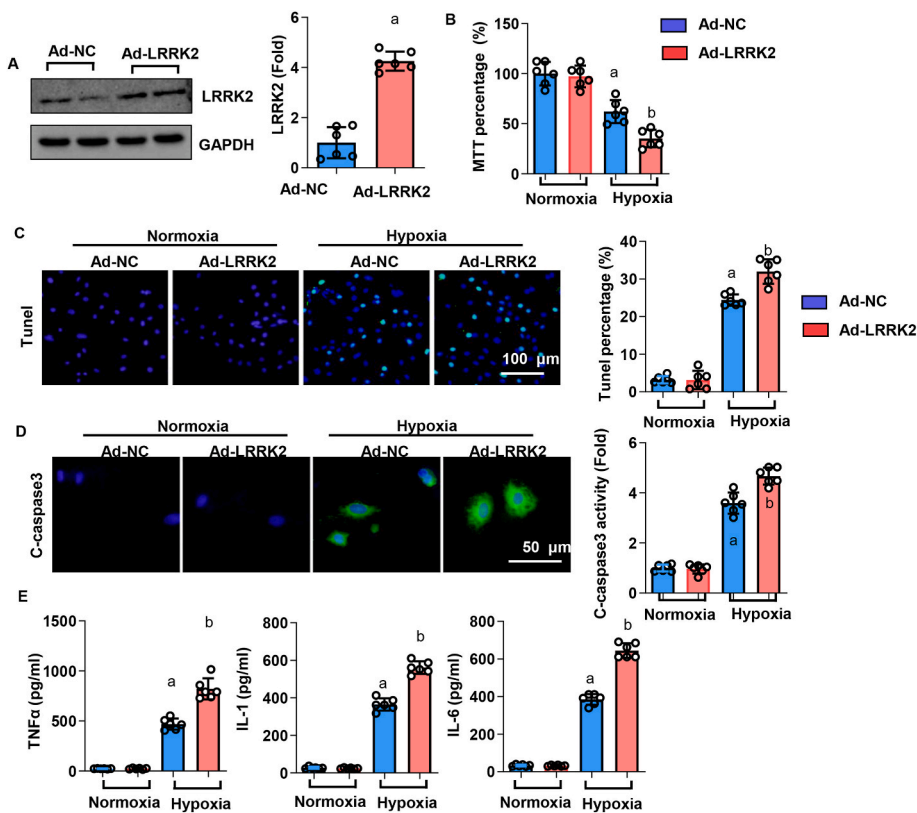


Fig. 3. LRRK2 overexpression worsens hypoxic cardiomyocyte injury
 A. Protein levels of LRRK2 in NRCMs after transfection with Ad-LRRK2 (n = 6). B. Cell viability after hypoxia for 24 h (n = 6). C. TUNEL staining and quantification of apoptotic cells (n = 5). D. c-caspase3 staining and activity (n = 6). F. ELISA analysis of proinflammatory cytokine concentrations (n = 6). ^aP < 0.05 vs. the Normoxia-Ad-NC group, ^bP < 0.05 vs. the hypoxia-Ad-NC group.

also higher than that in the Ad-NC group under hypoxic conditions (Fig. 3E).

3.4. LRRK2 deficiency in mice ameliorates heart MI injury and improves survival rate

It is unclear whether LRRK2 plays a role in the process by which cardiac remodelling after MI leads to HF. LRRK2-null mice (Fig. 4A) were subjected to LAD surgery to establish the MI model. Fourteen days after MI, the hearts were collected from the mice. We observed a reduction in the death rate in the LRRK2-null group during the 14 days of observation compared to the WT group (Fig. 4B). The myocardial infarction area was examined by HE staining, and we found that LRRK2 deficiency diminished the infarction area compared to that in the WT control group (Fig. 4C). PSR staining was used to examine LV fibrosis. As shown in Fig. 4D, the LV collagen volume in LRRK2-null mouse hearts was less than that in WT mouse hearts at 14 days after MI. As increased inflammatory cell infiltration and proinflammatory cytokine release lead to serious LV fibrosis and cardiac dysfunction, we explored the inflammatory response after MI. As shown in Fig. 4E and F, the number of CD68-positive macrophages and CD45-positive leucocytes was markedly reduced in LRRK2-deficient mice, and the concentration of proinflammatory cytokines in heart tissue was markedly abated compared with that in WT mice.

3.5. LRRK2 deficiency in mice improves cardiac function

Cardiac function was also examined by echocardiography and haemodynamic measurements. As shown in Fig. 5A and B, the LV end diastolic diameter (LVEDd) was increased and LV ejection fraction

(LVEF) and LV fractional shortening (LVFS) were reduced in WT mice 14 days after MI compared with sham mice, while these parameters were improved in LRRK2-null mice after MI. End diastolic left ventricular posterior wall thickness (LVPWd) was increased in both WT and KO mice after MI and showed no significant differences. Cardiac output was decreased in WT-MI mice but increased in KO-MI mice. Heart rate was not significantly different among the four groups (Fig. 5C). The heart mass and lung mass were increased in the MI group compared with the sham group, as evidenced by the heart weight- or lung weight-to-body weight ratios. These parameters were reduced in KO-MI mice compared with WT-MI mice (Fig. 5D).

3.6. LRRK2 affects the P53-HMGB1 pathway

We screened potential target and the upstream molecules of LRRK2. As a result, we found that the increase in LRRK2 expression in hypoxic cardiomyocytes was induced by HIF-1 α . Cells were treated with the HIF-1 α inhibitor KC7F2 (20 μ M) for 24 h. As shown in Fig. 6A, the expression of HIF-1 α was upregulated in NRCMs after hypoxia but decreased to baseline levels after treatment with KC7F2. The changes in LRRK2 expression were the same as those of HIF-1 α . When cells were treated with KC7F2, the hypoxia-induced increase in the expression level of LRRK2 was inhibited (Fig. 6A). HIF-1 α silence reduced the promoter activity of LRRK2 in cardiomyocytes (Fig. 6B). These results indicate that when cells suffer from hypoxia, high levels of HIF-1 α trigger the expression of LRRK2, which participates in the process of cardiac remodelling after MI. Next, we screened the potential targets of LRRK2. Studies have reported an effect of LRRK2 on the phosphorylation of P53, which plays a role in the release of HMGB1 [29]. We examined the protein level of P-P53 and found that P-P53 expression was upregulated

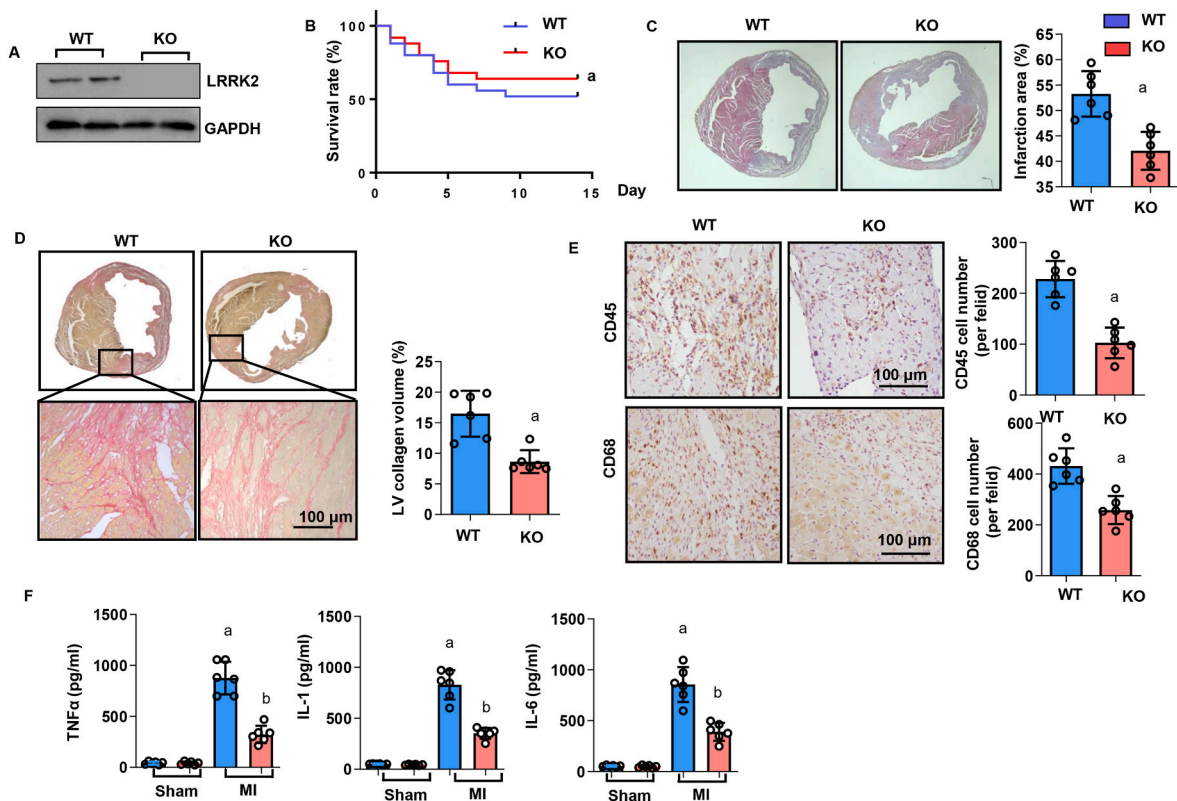


Fig. 4. LRRK2 deficiency in mice ameliorates MI injury and improves survival rates

A. Protein expression of LRRK2 in WT and KO mice (n = 6). B. Survival rates 14 days after MI (n = 25 per group). C. H&E staining and quantification of LV fraction areas (n = 6). D. PSR staining and quantification of LV collagen volumes (n = 6). E. CD45 and CD68 staining and quantification of CD45⁺ and CD68⁺ positive cell numbers (n = 6). F. ELISA analysis of proinflammatory cytokine concentrations in heart tissue (n = 6). ^aP < 0.05 vs. the WT-sham group, ^bP < 0.05 vs. the WT-MI group.

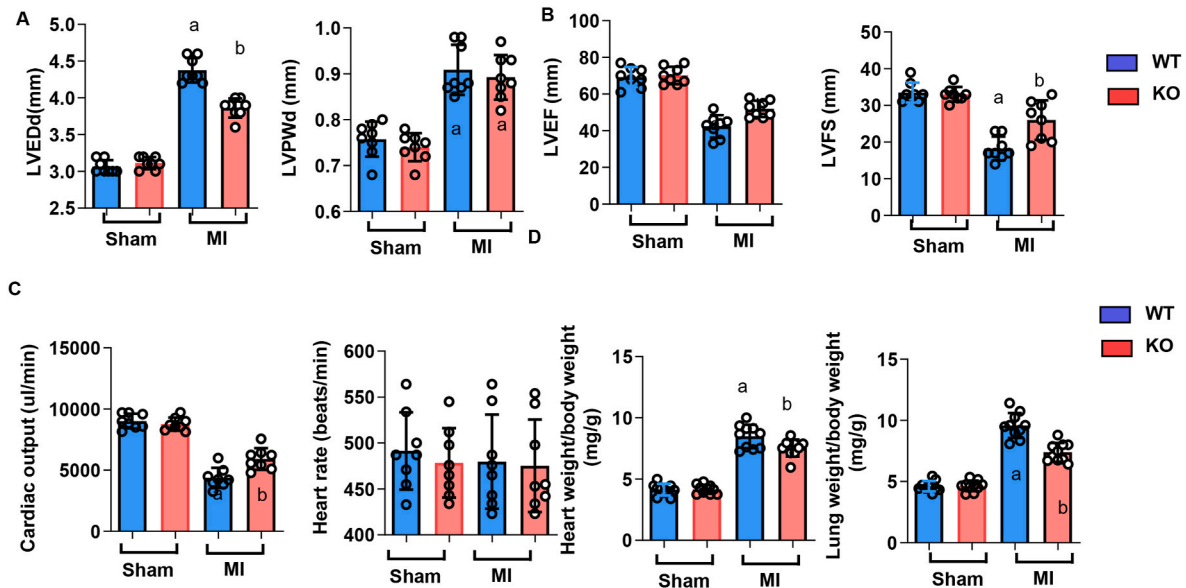


Fig. 5. LRRK2 deficiency in mice improves cardiac function

A and B. Echocardiography measurement of LVEDd, LVPWd, LVEF, and LVFS (n = 10). C. Haemodynamic measurement of cardiac output and heart rate (n = 10). D. Heart weight-to-body weight ratio, lung weight-to-body weight ratio (n = 10). ^aP < 0.05 vs. the WT-sham group, ^bP < 0.05 vs. the WT-MI group.

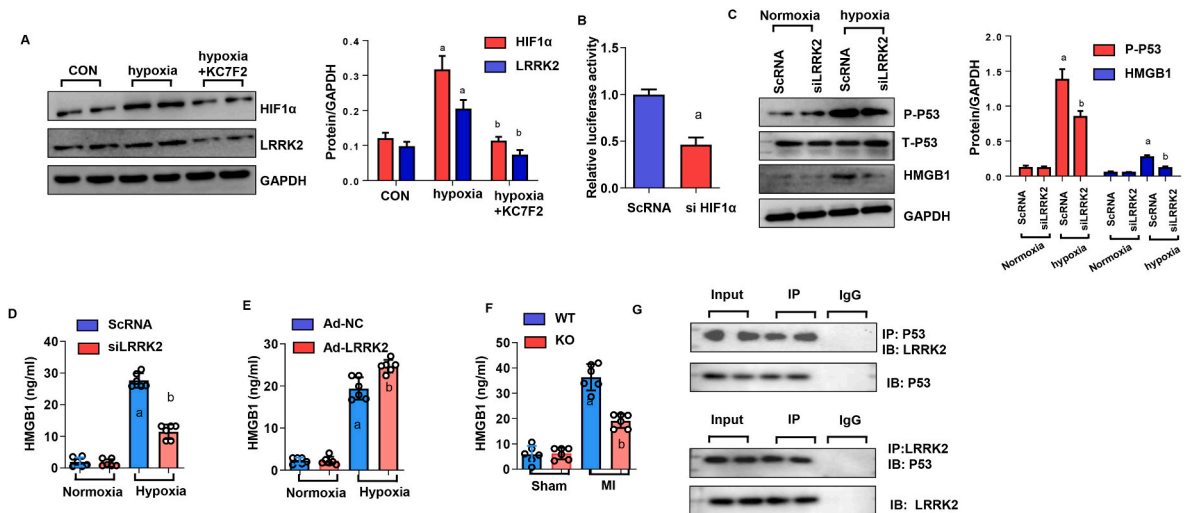


Fig. 6. LRRK2 affects the P53-HMGB1 pathway

A. NRCMs were treated with KC7F2 and exposed to hypoxia for 24 h. Protein levels of HIF-1 α and LRRK2 (n = 6). ^aP < 0.05 vs. the CON group, ^bP < 0.05 vs. the hypoxia group. B. Relative luciferase activity of LRRK2 in NRCMs transfected with HIF-1 α siRNA. ^aP < 0.05 vs. the ScRNA group. C. P53 and HMGB1 protein levels in NRCMs transfected with LRRK2 siRNA (n = 6). ^aP < 0.05 vs. the Normoxia-ScRNA group, ^bP < 0.05 vs. the hypoxia-ScRNA group. D-F. ELISA analysis of HMGB1 in NRCMs transfected with LRRK2 siRNA (n = 6, D ^aP < 0.05 vs. the Normoxia-ScRNA group, ^bP < 0.05 vs. the hypoxia-ScRNA group); in NRCMs transfected with Ad-LRRK2 (n = 6, E, ^aP < 0.05 vs. the Normoxia-Ad-NC group, ^bP < 0.05 vs. the hypoxia-Ad-NC group.); and in heart tissue (n = 6, F ^aP < 0.05 vs. the WT-sham group, ^bP < 0.05 vs. the WT-MI group). G. Co-IP analysis of NRCMs.

in NRCMs after hypoxia and downregulated by LRRK2 knockdown (Fig. 6C). Then, we examined the expression of HMGB1, which is a strong proinflammatory and proapoptotic DAMP. An increased in the HMGB1 level was observed in hypoxic NRCMs, while HMGB1 expression was downregulated in LRRK2-silenced cells (Fig. 6D). We further examined the concentration of HMGB1 in heart tissue after MI and in NRCMs after hypoxia. As shown in Fig. 6D–F, the concentration of HMGB1 was increased in both heart tissues after MI and cardiomyocytes after hypoxia; LRRK2 deficiency decreased the levels of HMGB1 in both ischaemic heart tissue and hypoxic cardiomyocytes, whereas LRRK2 overexpression increased the level of HMGB1 in hypoxic cardiomyocytes. Our co-IP results showed that LRRK2 could directly

interact with P53 (Fig. 6G).

3.7. LRRK2 kinase inhibition relieves hypoxic cardiomyocyte injury

Cells were also transfected with Ad-LRRK2 D1994A (kinase dead) [30] to confirm the effects of LRRK2 kinase on hypoxic cardiomyocyte injury. Hypoxia decreased cell viability and increased c-caspase3 activity and enhanced the release of TNF α , IL-1, and IL-6 in cardiomyocytes (Fig. 7A–C). However, cells in LRRK2 D1994A (kinase dead) overexpression group showed the same level of decreased cell viability, increased c-caspase3 activity and release of TNF α , IL-1, and IL-6 in cells under hypoxic conditions when compared with NC group

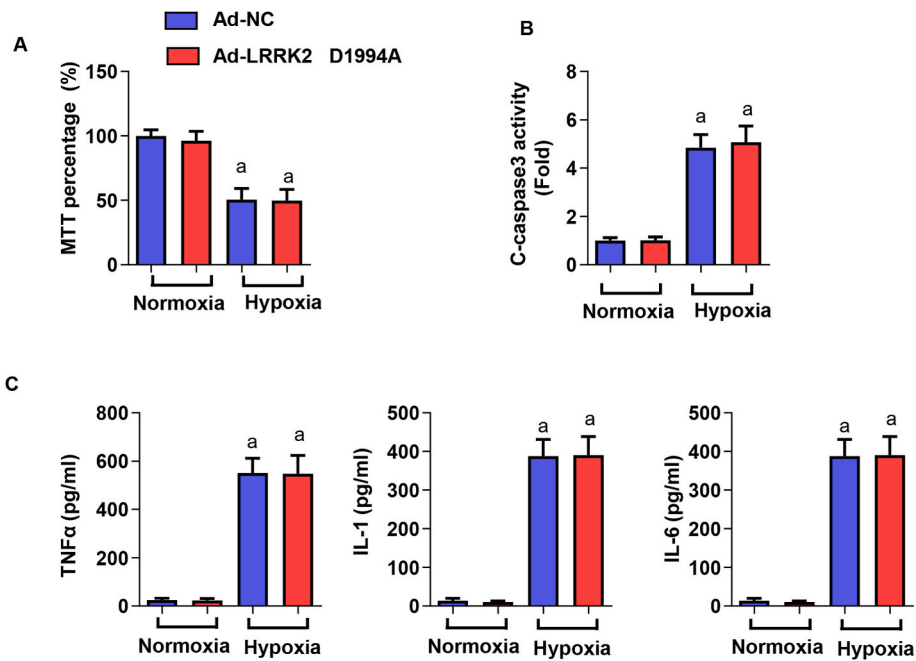


Fig. 7. LRRK2 kinase inhibition relieves hypoxic cardiomyocyte injury. NRCMs were transfected with LRRK2 D1994A (kinase dead). A. Cell viability after hypoxia for 24 h (n = 6). B. c-caspase3 staining and activity (n = 6). C. ELISA analysis of proinflammatory cytokine concentrations (n = 6). ^aP < 0.05 vs. the Normoxia-Ad-NC group, ^bP < 0.05 vs. the hypoxia-Ad-NC group.

(Fig. 7A–C).

3.8. HMGB1 antibodies counter the negative effects of LRRK2

We then used an HMGB1 antibody to block extracellular HMGB1 and

counteract the ligand effect of HMGB1. NRCMs were also transfected with Ad-LRRK2 to induce LRRK2 overexpression. As shown in Fig. 8A and B, cell viability was increased, and the number of TUNEL-positive cells was reduced in the anti-HMGB1 group compared to the hypoxia group. C-caspase3 expression and activity and proinflammatory

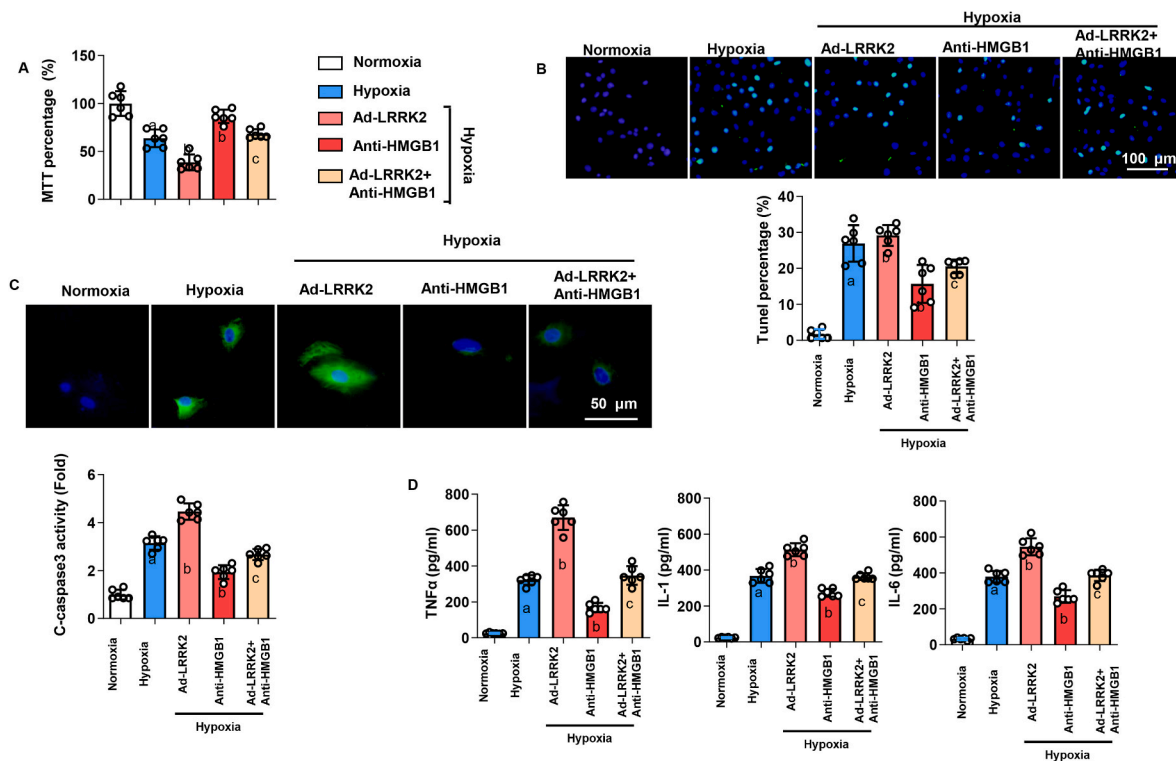


Fig. 8. The HMGB1 antibody counters the negative effects of LRRK2. A–D. NRCMs were transfected with Ad-LRRK2 and treated with anti-HMGB1 antibodies. A. Cell viability after hypoxia for 24 h (n = 6). B. TUNEL staining and quantification of apoptotic cells (n = 5). C. C-caspase3 staining and activity (n = 6). D. ELISA analysis of proinflammatory cytokine concentrations (n = 6). ^aP < 0.05 vs. the normoxia group, ^bP < 0.05 vs. the hypoxia group, ^cP < 0.05 vs. the Ad-LRRK2-hypoxia group.

cytokine concentrations were also reduced in the anti-HMGB1 group compared to the hypoxia group (Fig. 8C and D). The proapoptotic and proinflammatory effects of LRRK2 overexpression were counteracted by anti-HMGB1 antibody treatment, as shown by the reduced number of TUNEL-positive cells, reduced c-caspase3 activation and proinflammatory cytokine concentration, and increased cell viability in the Ad-LRRK2+anti-HMGB1 group (Fig. 8A–D).

4. Discussion

Myocardial infarction occurs when the coronary atherosclerotic plaque ruptures and the coronary arteries are completely occluded, causing ischaemia in the myocardium [8]. After myocardial infarction, a series of molecular, cellular, extracellular, and tissue changes occur in the left ventricle in surviving patients, who show clinical changes in heart size, structure, and function, ultimately leading to maladaptation (HF) [31]. The role of LRRK2, which had been previously studied as a PD-associated protein. Studies have reported that PD is a syndrome rather than a disease. In PD patients, it is usually found that parasympathetic nerve activity is decreased, while increased sympathetic nerve activity leads to cardiac changes, such as postural hypotension, decreased heart rate variability, changes in ECG parameters and baroreflex dysfunction, which worsen with the progress of the disease [32]. LRRK2 is associated with pathologies of PD with the mechanisms leading to neurodegeneration [33]. However, LRRK2 may also participate in cardiovascular disease independent of PD. We found that LRRK2 expression was upregulated in cardiac remodelling after MI and exerted deleterious effects on this process. The mRNA increased 2–3 times at 3 days after MI and 15–20 times at 7, 14 days post MI than in control group but the protein level increased 3 days after MI and maintain the same level at 7d, 14d post MI. Maybe more post-transcription modification and protein stability participate in the expression of LRRK2. During cardiac ischaemia, cardiomyocytes show increased HIF-1 α expression [34]. As a transcription factor, HIF-1 α regulates the expression of several molecules to compensate for oxygen and nutrient deprivation [34]. In our study, we observed that HIF-1 α increased the expression of LRRK2 during hypoxia, and a HIF-1 α inhibitor abrogated the hypoxia-induced upregulation of LRRK2.

MI is often fatal, and patients who survive acute myocardial infarction undergo an adaptive response to compensate for disordered haemodynamics and maintain cardiac function [31]. After the ischaemic attack, the loss of myocardial cells causes overloading of the ventricular wall, leading to dilatation of the ventricular chamber [7]. During this phase, the LVEF decreases abruptly, cardiac output decreases, and the LVEDV increases [7]. The body activates the sympathetic nervous system (SNS) and the renin-angiotensin-aldosterone system (RAAS) to compensate for the prolonged reduction in cardiac output [7]. In our study, we found that LRRK2 deficiency reduced the LVEDd and increased the LVEF, LVFS, and cardiac output at 14 days after MI. This finding suggests that LRRK2 deficiency may be beneficial in the adaptation of the heart to MI injury. After myocardial ischaemia leads to increased myocardial cell necrosis, a variety of immune cells, including neutrophils and monocytes, infiltrate the myocardial tissue to phagocytize dead cells [6]. Subsequently, the inflammatory phase subsides, the heart transitions to the repair and proliferative phase, and the factors secreted by inflammatory cells promote the proliferation of myofibroblasts and collagen deposition, leading to scar formation and mitochondrial damage [35,36]. Finally, a maturation process occurs, accompanied by the quiescence of myofibroblasts. A balance in the inflammation phase, proliferative phase, and maturation process is essential for the maintenance of cardiac function [6,31]. However, at 14 days after MI, we found that cardiac dysfunction in wild-type mice was accompanied by persistent inflammatory infiltration, inflammatory factor secretion, and fibrotic progression. Our previous study found that LRRK2 deficiency could protect against cardiac remodelling in mice post aortic banding [19]. In this study LRRK2 deficiency also found to

attenuate the increased inflammatory response, reduced inflammatory factor concentrations, and decreased collagen volume. LRRK2 deficiency also decreased the infarction area and improved the survival rate. In an *in vitro* study, LRRK2 overexpression enhanced cell apoptosis and the inflammatory response in response to hypoxia. This finding indicates that LRRK2 serves as a detrimental factor in cardiomyocytes under hypoxic conditions.

Cardiomyocyte death results in the massive release of DAMPs, which bind to pattern recognition receptors (PRRs) or TLRs, activating inflammatory signalling pathways [1]. HMGB1 is one of the most important DAMPs [9]. Under ischaemia or other stress, HMGB1 translocates from the nucleus to the cytoplasm through the Golgi/endoplasmic reticulum pathway, moves to the cell membrane and is finally secreted into the extracellular matrix [10]. Extracellular HMGB1 plays an important role in inflammation, apoptosis, necrosis, and autophagy [37]. HMGB1 binds to cell membrane receptors such as RAGE and TLR2/4 and induces the activation of NF- κ B and ERK1/2 signalling, triggering cells to produce proinflammatory cytokines [38]. In this study, we found that LRRK2 increased HMGB1 release in cardiomyocytes under hypoxia. LRRK2 deficiency decreased HMGB1 release in the ischaemic heart and cardiomyocytes. How did LRRK2 regulate HMGB1 release or expression? The transcription, translation, mRNA, and protein stability of HMGB1 are regulated by many molecules. Studies have shown that P53, CCAAT-binding transcription Factor 2 (CTF2), and JAK/STAT can regulate HMGB1 expression at the transcriptional level [39,40]. We found that LRRK2 silencing decreased HMGB1 protein levels. Ho DH et al. reported that LRRK2 could phosphorylate P53, leading to P53 activation in differentiated SH-SY5Y cells and microglial BV2 cells [29,41]. We examined the activation (phosphorylation) of P53 and found that LRRK2 deficiency reduced the level of P-P53 in cardiomyocytes. Thus, LRRK2 may regulate HMGB1 transcription via P53 activation. Previously, we found that LRRK2 regulates Bcl-2/Beclin1 and Rab7-regulated autophagy in cardiomyocytes under phenylephrine stimulation [19]. Here, in cardiomyocytes under hypoxia, LRRK2 regulated P53 associated cell death pathway. Autophagy was initially identified as a cell survival mechanism but it's also considered as type-II programmed cell death [42]. P53 also recognised as a regulator for all types of cell death including autophagy [43]. Moreover, under myocardial ischaemia, cells die more in the form of apoptosis. Thus, LRRK2 may regulate different type of cardiomyocytes death when cells under different stress.

In summary, our study demonstrated that during ischaemic conditions, high levels of HIF-1 α stimulate LRRK2 expression, which promotes P53 phosphorylation and activation, causing the transcription of HMGB1. The increased release of HMGB1 accelerates inflammation and apoptosis in the ischaemic heart, which leads to HF. Thus, targeting LRRK2 may become a new therapeutic strategy for inhibiting the progression of cardiac remodelling after MI.

Ethics approval

The Guide for the Care and Use of Laboratory Animals published by the US National Institutes of Health (NIH Publication No. 85-23, revised 1996) and the ARRIVE guidelines and the Animal Care and Use Committee of Zhengzhou University guided our study.

Sources of funding

This study was supported by the National Natural Science Foundation of China (Grant nos. 82070233, 82100252), the Scientific and Technological Project of Henan Province (202102310364).

Authors' contribution

Liu Yuan and Li Ran contributed to the conception and design of the experiments; Chen Lu and Gao lu carried out the experiments; Pei Xiao-

xin, Tao Ze-kai and Xu Ya-wei analysed the experimental results and revised the manuscript; Liu Yuan wrote and revised the manuscript.

Availability of data and material

The original data will be available when requiring to the corresponding author.

Declaration of competing interest

The authors declare no conflicts of interest.

Data availability

The authors do not have permission to share data.

Appendix A. Supplementary data

Supplementary data to this article can be found online at <https://doi.org/10.1016/j.freeradbiomed.2022.08.035>.

References

- [1] M. Jung, M. D. T. Thum, Inflammatory cells and their non-coding RNAs as targets for treating myocardial infarction, *Basic Res. Cardiol.* 114 (1) (2018) 4.
- [2] D.M. Musher, M.S. Abers, V.F. Corrales-Medina, Acute infection and myocardial infarction, *N. Engl. J. Med.* 380 (2) (2019) 171–176.
- [3] W.C. Stanley, Cardiac energetics during ischaemia and the rationale for metabolic interventions, *Coron. Artery Dis.* 12 (Suppl 1) (2001) S3–S7.
- [4] M.C. Marc, et al., Microvascular obstruction in acute myocardial infarction: an old and unsolved mystery, *Med Pharm Rep* 92 (3) (2019) 216–219.
- [5] A. Farah, A. Barbagelata, Unmet goals in the treatment of acute myocardial infarction: review, *F1000Res* 6 (2017).
- [6] B.R. Weil, S. Neelamegham, Selectins and immune cells in acute myocardial infarction and post-infarction ventricular remodeling: pathophysiology and novel treatments, *Front. Immunol.* 10 (2019) 300.
- [7] D. Gabriel-Costa, The pathophysiology of myocardial infarction-induced heart failure, *Pathophysiology* 25 (4) (2018) 277–284.
- [8] R.O. Mouton AJ, M.L. Lindsey, Myocardial infarction remodeling that progresses to heart failure: a signaling misunderstanding, *Am. J. Physiol. Heart Circ. Physiol.* 315 (1) (2018) H71–H79.
- [9] H. Lu, et al., Dual faced HMGB1 plays multiple roles in cardiomyocyte senescence and cardiac inflammatory injury, *Cytokine Growth Factor Rev.* 47 (2019) 74–82.
- [10] L. Pellegrini, et al., HMGB1 and repair: focus on the heart, *Pharmacol. Ther.* 196 (2019) 160–182.
- [11] P. Asavarut, et al., The role of HMGB1 in inflammation-mediated organ injury, *Acta Anaesthesiol. Taiwanica* 51 (1) (2013) 28–33.
- [12] W. Gao, et al., Upregulation of microRNA-218 Reduces Cardiac Microvascular Endothelial Cells Injury Induced by Coronary Artery Disease through the Inhibition of HMGB1, *J Cell Physiol*, 2019.
- [13] F.D. Liu FY, Z. Yang, N. Tang, Z. Guo, S.Q. Ma, Z.G. Ma, H.M. Wu, W. Deng, Q. Z. Tang, TLR9 is essential for HMGB1-mediated post-myocardial infarction tissue repair through affecting apoptosis, cardiac healing, and angiogenesis, *Cell Death Dis.* 10 (7) (2019) 480.
- [14] Z. hu, X. H. Z. Fang, S. Zhou, Endothelial cell is critical in HMGB1 mediated cardiac impairment in ischemic heart disease, *Int. J. Cardiol.* 187 (2015) 39–40.
- [15] Z. Su, et al., Up-regulated HMGB1 in EAM directly led to collagen deposition by a PKCbeta/Erk1/2-dependent pathway: cardiac fibroblast/myofibroblast might be another source of HMGB1, *J. Cell Mol. Med.* 18 (9) (2014) 1740–1751.
- [16] M. Rassu, et al., Levetiracetam treatment ameliorates LRRK2 pathological mutant phenotype, *J. Cell Mol. Med.* 23 (12) (2019) 8505–8510.
- [17] Y. Tian, et al., LRRK2 plays essential roles in maintaining lung homeostasis and preventing the development of pulmonary fibrosis, *Proc. Natl. Acad. Sci. U. S. A.* 118 (35) (2021).
- [18] T. Takagawa, et al., An increase in LRRK2 suppresses autophagy and enhances Dectin-1-induced immunity in a mouse model of colitis, *Sci. Transl. Med.* 10 (444) (2018).
- [19] Y. Liu, et al., Leucine-rich repeat kinase-2 deficiency protected against cardiac remodelling in mice via regulating autophagy formation and degradation, *J. Adv. Res.* 37 (2022) 107–117.
- [20] C. Ren, et al., G2019S variation in LRRK2: an ideal model for the study of Parkinson's disease? *Front. Hum. Neurosci.* 13 (2019) 306.
- [21] C. Rudyk, et al., Leucine-rich repeat kinase-2 (LRRK2) modulates paraquat-induced inflammatory sickness and stress phenotype, *J. Neuroinflammation* 16 (1) (2019) 120.
- [22] C.J. Gu S, Q. Zhou, M. Yan, J. He, X. Han, Y. Qiu, LRRK2 Is Associated with Recurrence-free Survival in Intrahepatic Cholangiocarcinoma and Downregulation of LRRK2 Suppresses Tumor Progress in Vitro, *Dig Dis Sci*, 2019 ([Epub ahead of print]).
- [23] Z.C. Jiang, et al., Downregulated LRRK2 gene expression inhibits proliferation and migration while promoting the apoptosis of thyroid cancer cells by inhibiting activation of the JNK signaling pathway, *Int. J. Oncol.* 55 (1) (2019) 21–34.
- [24] M.H.R. Ludtmann, et al., LRRK2 deficiency induced mitochondrial Ca(2+) efflux inhibition can be rescued by Na(+)/Ca(2+)/Li(+) exchanger upregulation, *Cell Death Dis.* 10 (4) (2019) 265.
- [25] Y. Liu, et al., Toll-like receptor 5 deficiency attenuates interstitial cardiac fibrosis and dysfunction induced by pressure overload by inhibiting inflammation and the endothelial-mesenchymal transition, *Biochim. Biophys. Acta* 1852 (11) (2015) 2456–2466.
- [26] Y. Liu, et al., Saikosaponin A protects from pressure overload-induced cardiac fibrosis via inhibiting fibroblast activation or endothelial cell EndMT, *Int. J. Biol. Sci.* 14 (13) (2018) 1923–1934.
- [27] Y. Gu, et al., Bcl6 knockdown aggravates hypoxia injury in cardiomyocytes via the P38 pathway, *Cell Biol. Int.* (2018).
- [28] Q.Q. Wu, et al., OX40 regulates pressure overload-induced cardiac hypertrophy and remodelling via CD4+ T-cells, *Clin. Sci. (Lond.)* 130 (22) (2016) 2061–2071.
- [29] D.H. Ho, et al., Phosphorylation of p53 by LRRK2 induces microglial tumor necrosis factor alpha-mediated neurotoxicity, *Biochem. Biophys. Res. Commun.* 482 (4) (2017) 1088–1094.
- [30] E.H. Howlett, et al., LRRK2 G2019S-induced mitochondrial DNA damage is LRRK2 kinase dependent and inhibition restores mtDNA integrity in Parkinson's disease, *Hum. Mol. Genet.* 26 (22) (2017) 4340–4351.
- [31] N.S. Dhalla, et al., Cardiac remodeling and subcellular defects in heart failure due to myocardial infarction and aging, *Heart Fail. Rev.* 17 (4–5) (2012) 671–681.
- [32] L. Cuenca-Bermejo, et al., Cardiac changes in Parkinson's disease: lessons from clinical and experimental evidence, *Int. J. Mol. Sci.* 22 (24) (2021).
- [33] G.R. Jeong, B.D. Lee, Pathological functions of LRRK2 in Parkinson's disease, *Cells* 9 (12) (2020).
- [34] D. Tekin, A.D. Dursun, L. Xi, Hypoxia inducible factor 1 (HIF-1) and cardioprotection, *Acta Pharmacol. Sin.* 31 (9) (2010) 1085–1094.
- [35] W. Yu, et al., TBC1D15/RAB7-regulated mitochondria-lysosome interaction confers cardioprotection against acute myocardial infarction-induced cardiac injury, *Theranostics* 10 (24) (2020) 11244–11263.
- [36] M. Sun, et al., NDP52 Protects against Myocardial Infarction-Provoked Cardiac Anomalies through Promoting Autophagosome-Lysosome Fusion via Recruiting TBK1 and RAB7, *Antioxid Redox Signal*, 2021.
- [37] H.S. Ding, et al., The HMGB1-TLR4 axis contributes to myocardial ischemia/reperfusion injury via regulation of cardiomyocyte apoptosis, *Gene* 527 (1) (2013) 389–393.
- [38] M. Takahashi, High-mobility group box 1 protein (HMGB1) in ischaemic heart disease: beneficial or deleterious? *Cardiovasc. Res.* 80 (1) (2008) 5–6.
- [39] M. Stros, et al., HMGB1-mediated DNA bending: distinct roles in increasing p53 binding to DNA and the transactivation of p53-responsive gene promoters, *Biochim Biophys Acta Gene Regul Mech* 1861 (3) (2018) 200–210.
- [40] G. Verrijdt, et al., Comparative analysis of the influence of the high-mobility group box 1 protein on DNA binding and transcriptional activation by the androgen, glucocorticoid, progesterone and mineralocorticoid receptors, *Biochem. J.* 361 (Pt 1) (2002) 97–103.
- [41] D.H. Ho, et al., Leucine-Rich Repeat Kinase 2 (LRRK2) phosphorylates p53 and induces p21(WAF1/CIP1) expression, *Mol. Brain* 8 (2015) 54.
- [42] S. Dadakhujaev, et al., Interplay between autophagy and apoptosis in TrkA-induced cell death, *Autophagy* 5 (1) (2009) 103–105.
- [43] V. Nikolettou, et al., Crosstalk between apoptosis, necrosis and autophagy, *Biochim. Biophys. Acta* 1833 (12) (2013) 3448–3459.